Supporting Information

For

Perylene diimide-based radical anion for the rapid detection of picomolar H_2O_2 in aqueous medium

Navdeep Kaur[a], Sagar Sardana[b], Aman Mahajan[b], Subodh Kumar[a] and Prabhpreet Singh[*a]

Department of Chemistry, UGC Centre for Advanced Studies-II, Guru Nanak Dev University, Amritsar 143001 (pb.)-India E-mail: prabhpreet.chem@gndu.ac.in; M: +91 8427101534

Department of Physics, Guru Nanak Dev University, Amritsar 143001 (pb.)-India

EXPERIMENTAL SECTION

Methods and Instrumentations: The reagent grade chemicals such as 4-formylphenylboronic acid, nitromethane, ammonium acetate, glacial acetic acid and $Pd(PPh_3)_4$ were procured from Sigma Aldrich, Tokyo Chemical Industries (TCI) and Spectrochem Pvt. Ltd., India and used without further purification. The HPLC grade tetrahydrofuran (THF), toluene and water were used for analytical studies. Chloroform was used after distillation for organic synthesis and in column chromatography for purification of organic compounds. All reactions were performed under N_2 stream. Thin layer chromatography (TLC) for monitoring the progress of the reactions was performed on aluminum sheets coated with silica gel 60 F254 (Merck, Darmstadt, Germany). The HEPES buffer (2.38 g) was dissolved in 1 L deionized water and pH of the buffer was adjusted to *ca*. 7.4. Preparative liquid chromatography (PLC) was performed on glass plates. All spectroscopic measurements were carried out in THF and 10–50% HEPES buffer–THF solution at 10 or 20 μM concentrations of neutral PDI **1** at room temperature.

The proton (^1H) and carbon (^{13}C) NMR spectra were recorded on BRUKER Biospin AVANCE-III FT-NMR HD-500 spectrometer in $CDCl_3$ and referenced to tetramethyl silane (TMS) as an internal standard for ^1H and residual signals for ^{13}C. The spin multiplicities are reported as (s = singlet, d = doublet, t = triplet, q = quartet, dd = doublet of doublet and m = multiplet) with coupling constants (*J*) values in Hz. The FT-IR (ATR) spectra were recorded on the Perkin Elmer 92035 spectrometer. The absorbance studies were carried out on Cary 5000 UV-VIS-NIR spectrophotometer equipped with a Peltier to control the temperature. The UV-VIS-NIR spectra of different solutions of neutral PDI **1** in THF and binary mixtures of THF–H_2O in the absence and presence of different analytes were recorded in quartz cells having 1 cm path length, 2 nm band width and 140 nm min^{-1} scan rate. The fluorescence spectra of different solutions of neutral PDI **1** in THF and binary mixtures of THF–H_2O in the absence and presence of different analytes were recorded using RF 6000 SHIMADZU Spectrofluorophotometer. The cyclic voltammetry (CV) and differential pulse voltammetry (DPV) experiments of neutral PDI **1** in the absence and presence of different

concentrations of H_2S and H_2O_2 were performed on Metrohm Autolab PGSTAT302N electrochemical workstation at room temperature using a standard three electrode arrangement that consists of platinum electrode as both working and auxiliary electrodes and Ag/AgCl (saturated with KCl solution) as reference electrode. All the electrochemical measurements were carried out after purging N_2 gas. Tetrabutylammonium hexafluorophosphate was used as the supporting electrolyte. The AFM micrographs were recorded on a Tosca 400 instrument developed by Anton Paar to characterize the topography of neutral PDI **1** and neutral PDI **1**+H_2S. Two probe Agilent B2902A precision measurement unit source meter was used to measure the resistance and data was analyzed using a computer equipped with quick I–V software. The change in resistance was recorded as a function of time at different potentials. All the sensing measurements have been performed under 30–40% relative humidity. FE-SEM measurements were performed on a ZEISS SUPRA^{TM} 55, operating at an acceleration voltage of 10 kV with a tungsten filament (electron source). Sputtering of dried samples was performed with silver prior to FE-SEM imaging. The theoretical calculation of neutral PDI **1** and PDI $\mathbf{1}^{\bullet-}$ have been performed with the Gaussian 09 package using density functional theory (DFT) and time dependent density functional theory (TD-DFT) at B3LYP/6-31G* level.

Synthesis of PDI-CHO

To a solution of **PDI-Br** (1 g, 1.6 mmol) in toluene (12 ml) with purging of N_2 gas, Na_2CO_3 (0.9 mmol), tetrakis-(triphenylphosphine)palladium (10 mol%) and 4-formylphenylboronic acid (1.6 mmol) were added. Now, ethanol and water (1:1) was added to reaction mixture and stirred for 7-8h at 80 °C. After completion of the reaction (*tlc*), solvent was removed from the reaction mixture and organic residue was extracted with chloroform (2x50 ml). The chloroform layer was washed with brine, dried over Na_2SO_4 and concentrated on rotary evaporator to isolate crude residue which was purified by column chromatography using $CHCl_3$: hexane (99:1, v/v) as mobile mixture to isolate PDI-**CHO** as a bright red solid; Yield 81.7%; R_f = 0.52; ^{1}H NMR (500 MHz, CDCl3, 25°C): δ 0.88-0.94 (2t merged, 12H, 4xCH_3), 1.89-1.95 (m, 4H, 2xCH_2), 2.21-2.29 (m, 4H, 2xCH_2), 5.00-5.11 (s, 2H, N-CH), 7.71 (d, 2H, *J* = 7 Hz, Phenyl-ArH), 7.76 (d, 1H, *J* = 8.5 Hz, Perylene-ArH), 8.06 (d, 2H, *J* = 7.5 Hz, Phenyl-ArH), 8.12 (d, 1H, *J* = 8 Hz, Perylene-ArH), 8.56 (s, 1H, Perylene-ArH), 8.64- 8.73 (m, 4H, Perylene-ArH), 10.15 (s, 1H, CHO) ppm; ^{13}C NMR (125 MHz, $CDCl_3$, 25 °C): δ 11.44, 25.09, 25.13, 57.79, 57.94, 123.13, 123.86, 127.55, 128.16, 128.91, 129.30, 129.66, 130.42, 131.69, 132.91, 134.15, 134.33, 134.98, 136.17, 140.06, 148.89, 191.54 ppm; HRMS: Calculated for $C_{41}H_{34}N_2O_5$+Na^+ = 657.2365; found = 657.2319.

Synthesis of PDI 1

To a solution of **PDI-CHO** (0.2 g, 0.32 mmol) in nitromethane (4.3 ml), CH_3COONH_4 (0.22 g, 0.95 mmol) and CH_3COOH (1.14 ml) were added and reaction mixture was stirred for 3h at 80 °C. After completion of the reaction (*tlc*), water was added to the reaction mixture and organic residue was extracted with chloroform (2x50 ml). The chloroform layer was washed with brine, dried over Na_2SO_4 and concentrated on rotary evaporator to isolate crude residue which was purified by column chromatography using $CHCl_3$: hexane (98:2, v/v) mixture as eluent to isolate PDI **1** as a bright red solid; Yield 85%; R_f = 0.6; ^{1}H NMR (500 MHz, $CDCl_3$, 25°C): δ 0.89-0.95 (two triplets merged, 12H, 4xCH_3), 1.90–1.96 (m, 4H, 2xCH_2), 2.21–2.29 (m, 4H, 2xCH_2), 5.01–5.10 (s, 2H, NCH), 7.62 (d, 2H, *J* = 8 Hz, ArH), 7.70 (d, 1H, *J* = 14 Hz, =CH), 7.74 (d, 2H, *J* = 8 Hz, ArH), 7.81 (d, 1H, *J* = 8 Hz, Perylene ArH), 8.10 (d, 1H, *J* = 13.5 Hz, =CH), 8.14 (d, 1H, *J* = 8 Hz, Perylene ArH), 8.55 (s, 1H, Perylene ArH), 8.62–8.72 (m, 4H, Perylene ArH) ppm; ^{13}C NMR (125 MHz, $CDCl_3$, 25 °C): δ 11.43, 25.08, 25.12, 57.79, 57.93, 123.11, 123.88, 127.56, 128.11, 128.18, 128.86, 129.30, 129.97, 130.10, 130.29, 130.44, 131.11, 132.87, 134.23, 134.35, 134.61, 134.94, 137.49, 138.00, 138.36, 140.01, 143.24, 146.54 ppm; IR (ATR): ν = 2922.2, 2363.1, 2109.7, 1915.9, 1654.9, 1587.8, 1520.8, 1461.1, 1326.9, 1237.5, 1080.9, 969.1, 849.8 cm^{-1}; HRMS: Calculated for ($C_{42}H_{35}N_3O_6$+Na) = 700.2418; found = 700.2000; ($C_{42}H_{35}N_3O_6$)x2 + Na^+ = 1377.4944 found 1377.3795; ($C_{42}H_{35}N_3O_6$)x3 + Na^+ = 2054.7470 found 2054.5407.

General procedure for formation of radical anion

The solutions of neutral PDI **1** (10 μM) were prepared in THF and in binary mixtures of 10–50% HEPES buffer–THF (pH 7.4). The freshly prepared solution of H_2S (0.1 M) was added at different concentrations to neutral PDI **1** solution. The immediate formation of radical anion (PDI $\mathbf{1}^{\bullet-}$) was observed. PDI $\mathbf{1}^{\bullet-}$ is stable in oxygenated aqueous medium. The PDI $\mathbf{1}^{\bullet-}$ was freshly generated before conducting each different spectroscopic measurement.

Thin film preparations and sensor fabrication

The electrical conductivity studies for PDI **1** and PDI $\mathbf{1}^{\bullet-}$ were based on direct current-voltage (I-V) measurements from thin films. The flat surface of glass plate is highly suitable for fabrication of flat electrodes and compound deposition. Therefore, 30 μL of neutral PDI **1** and PDI $\mathbf{1}^{\bullet-}$ solutions (prepared in 50% HEPES buffer–THF) were deposited on the glass plate by drop casting technique, followed by drying in oven at 60 °C. The solvent such as THF and HEPES buffer solution used in thin film preparations were pre-filtered through a Millipore membrane filter (Acrodisc syringe filter, 0.2 μm Supor membrane). Subsequently, the sensors were fabricated by depositing Ag paste electrode at a distance of 1 cm on thin film samples followed by drying at 60 °C for 30 mins. prior to their use for I-V sensing.

Procedure for detection of H_2O_2

To the solution of PDI **1**$^{\bullet-}$ (generated in situ upon addition of 8 mM H_2S in neutral PDI **1**) in 50% HEPES buffer–THF (pH 7.4), different concentrations of H_2O_2 (0–1.5 nM) were added and absorbance spectra were recorded.

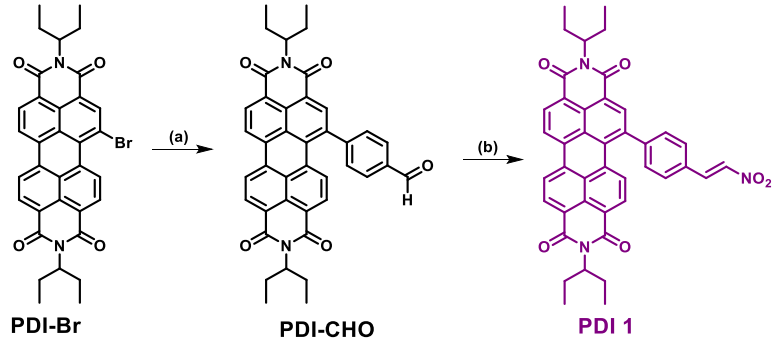

Scheme S1. Synthesis of PDI **1**: *Reagents and conditions*: (a) Na_2CO_3, $Pd(PPh_3)_4$, 4-formylphenyl boronic acid, ethanol-H_2O (1:1), toluene, (b) nitromethane, CH_3COONH_4, anhydrous glacial acetic acid, 80 ^oC, 6h.

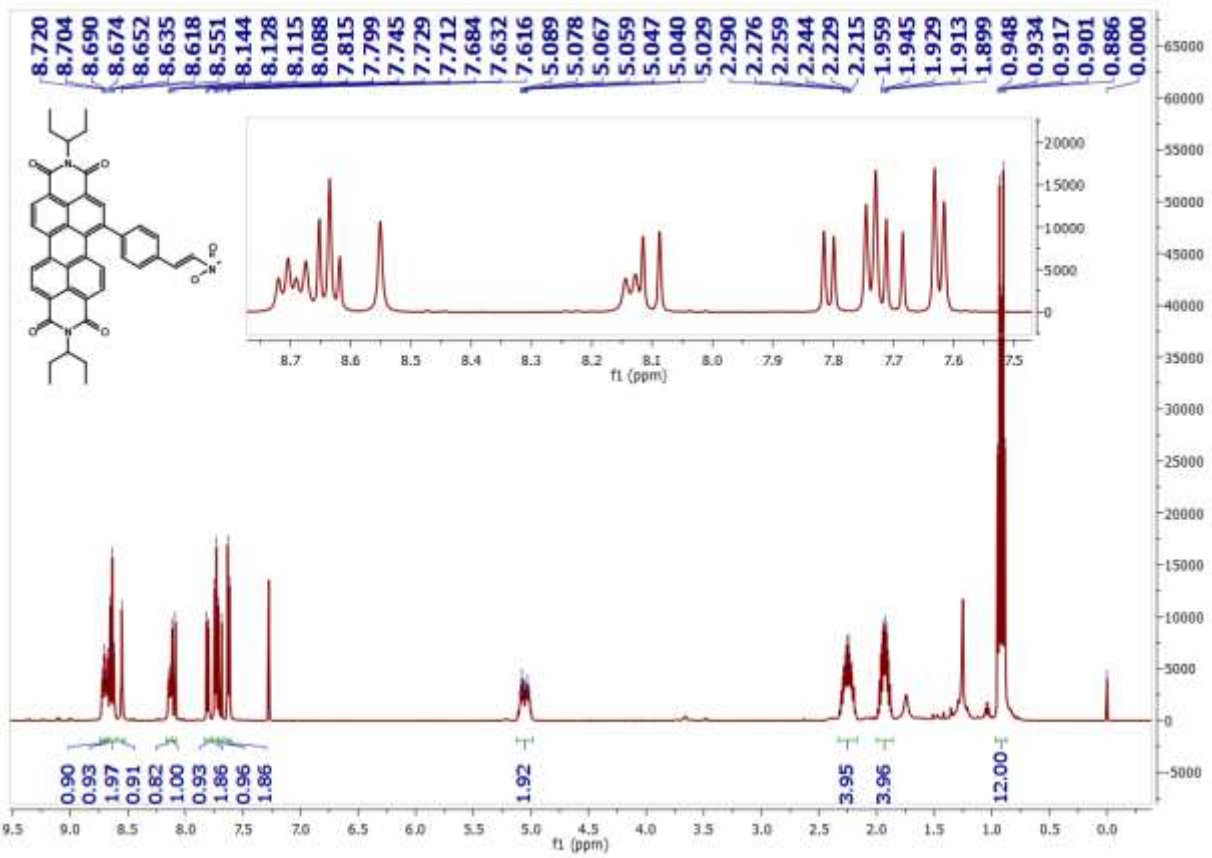

Figure 1a. The Proton (^1H) NMR spectrum for PDI **1**.

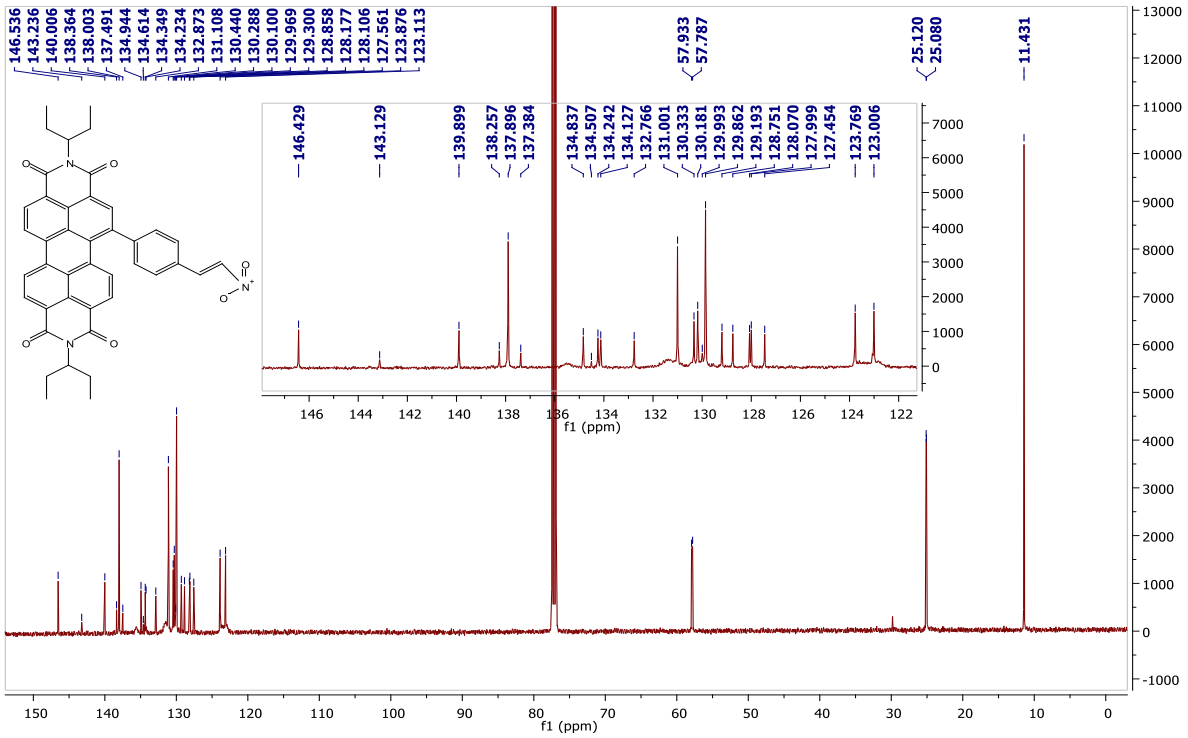

Figure 1b. The Carbon (^{13}C) NMR spectrum for PDI **1**.

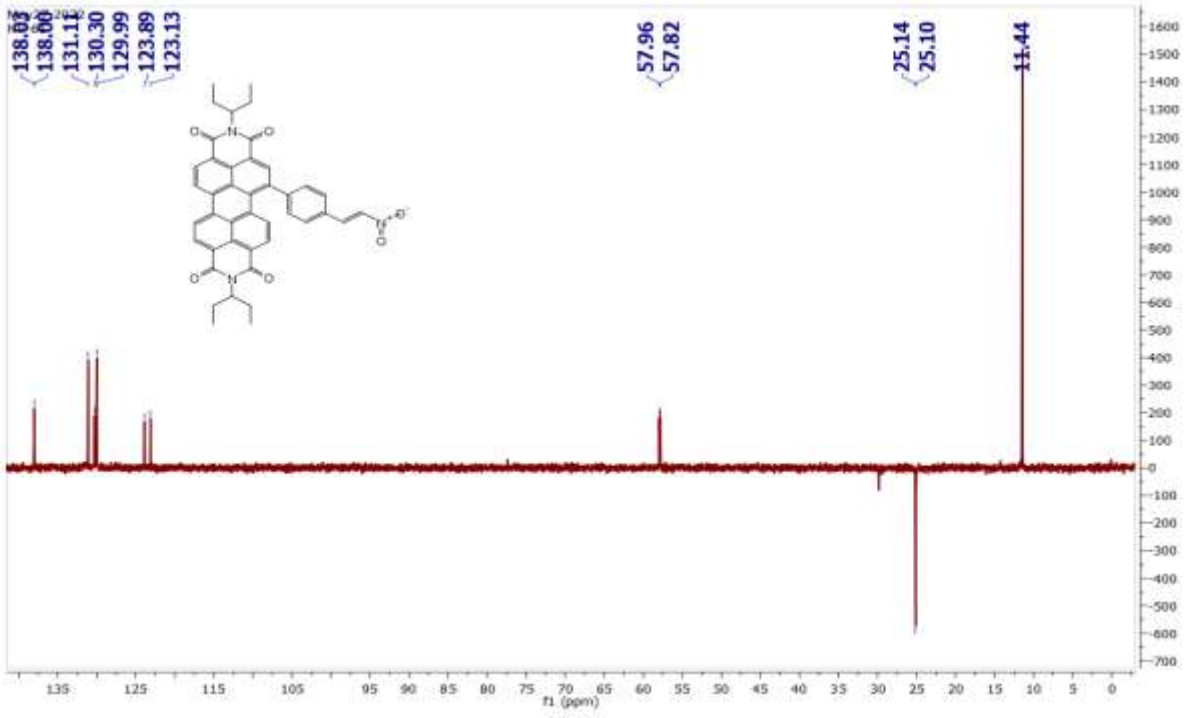

Figure 1c. The Carbon DEPT-135 NMR spectrum for PDI **1**.

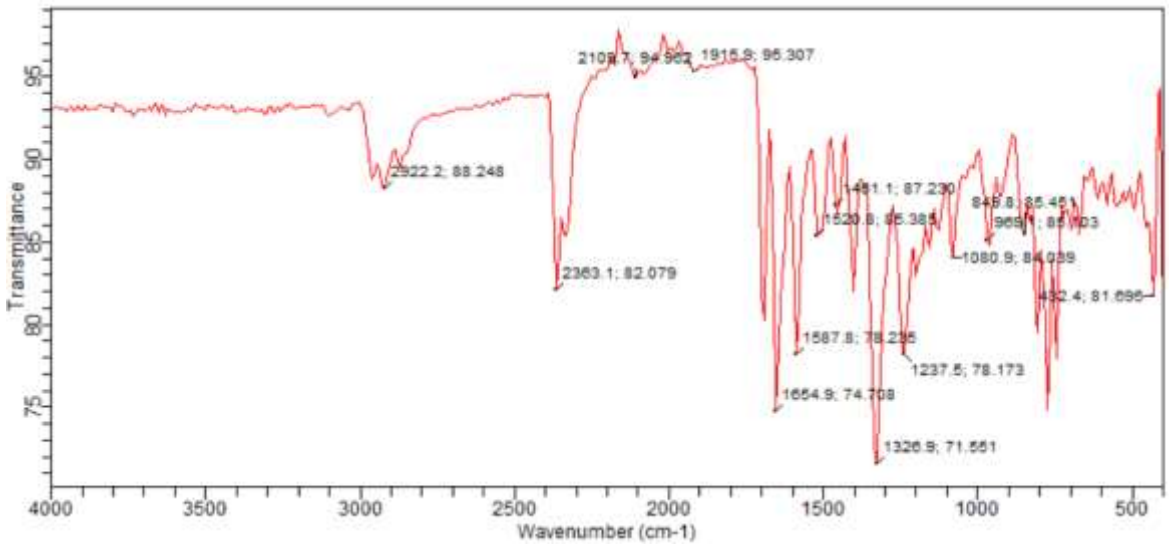

Figure 1d. FTIR (ATR) spectrum for PDI **1**.

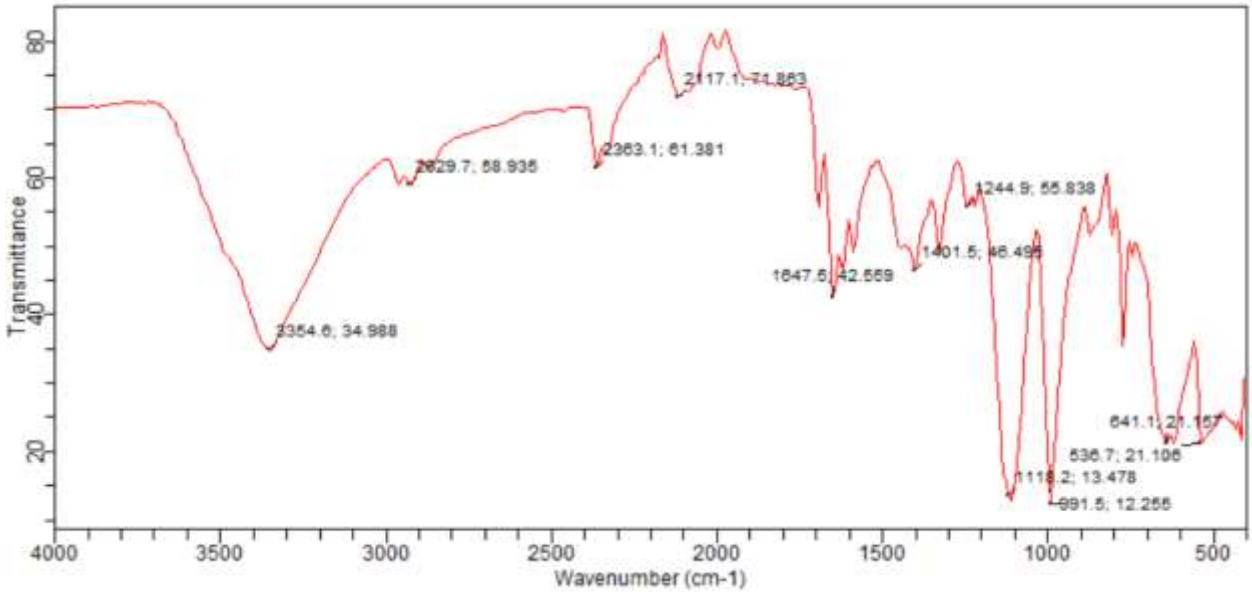

Figure S1e. FTIR (ATR) spectrum for PDI 1 radical.

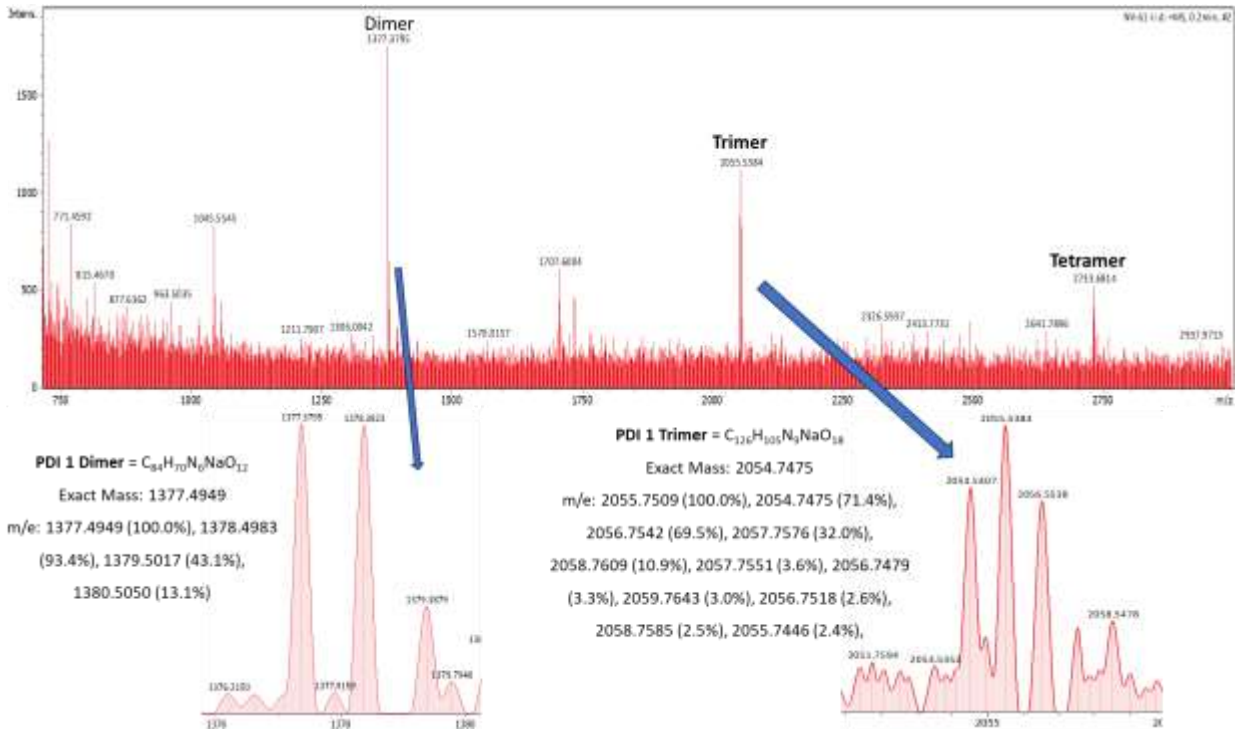

Figure S1f. Mass spectrum of PDI **1.**

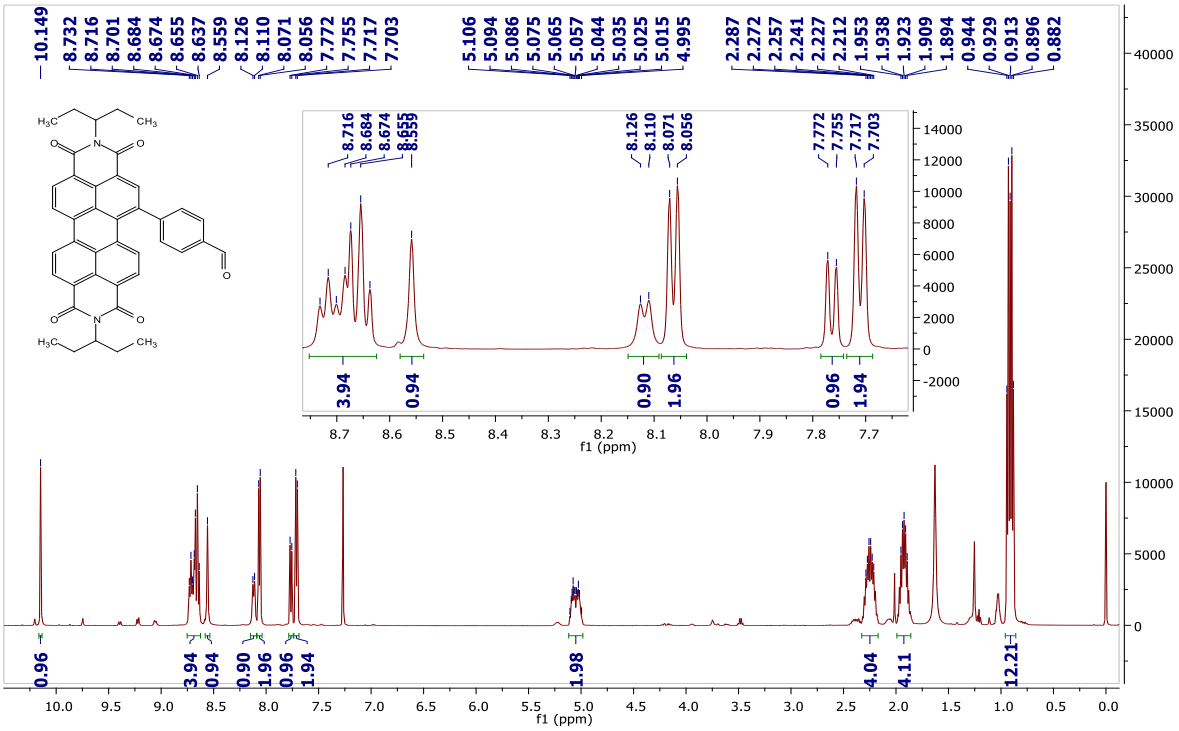

Figure S2a. The Proton (^{1}H) NMR spectrum for PDI-CHO.

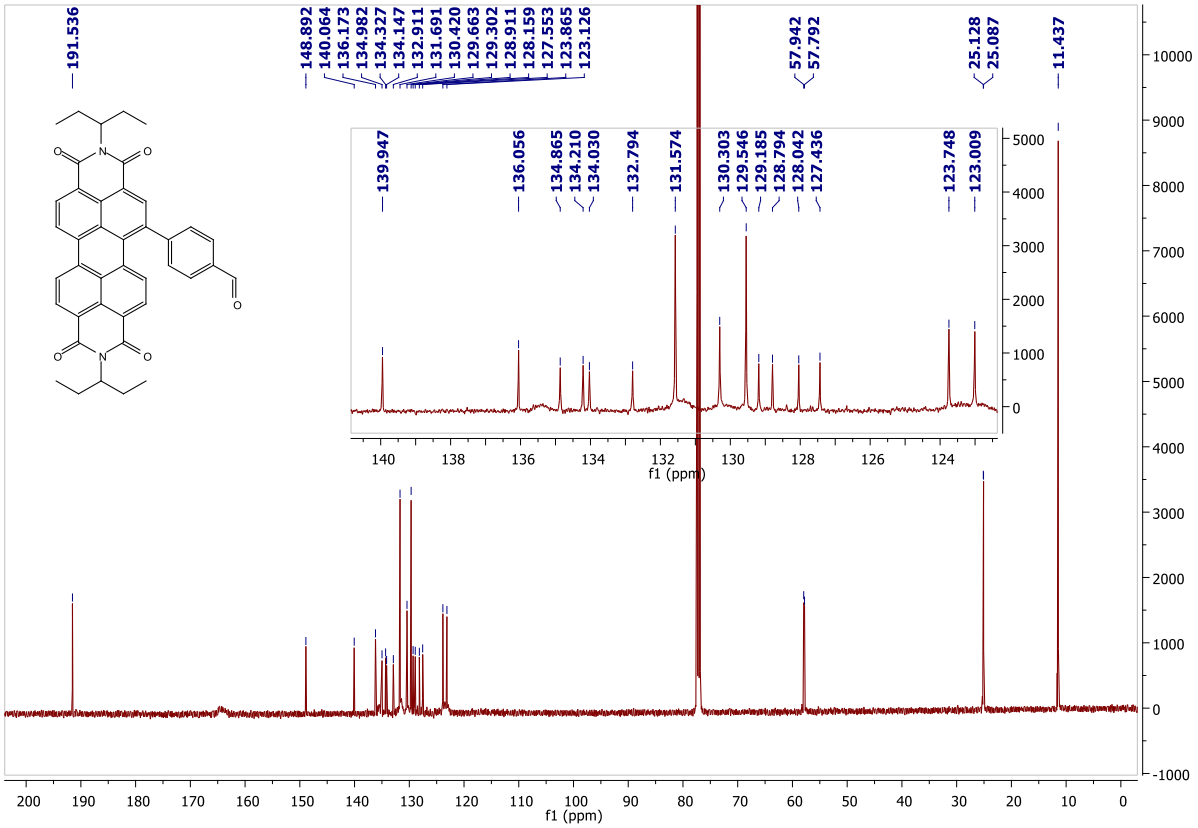

Figure S2b. The Carbon (^{13}C) NMR spectrum for PDI-CHO.

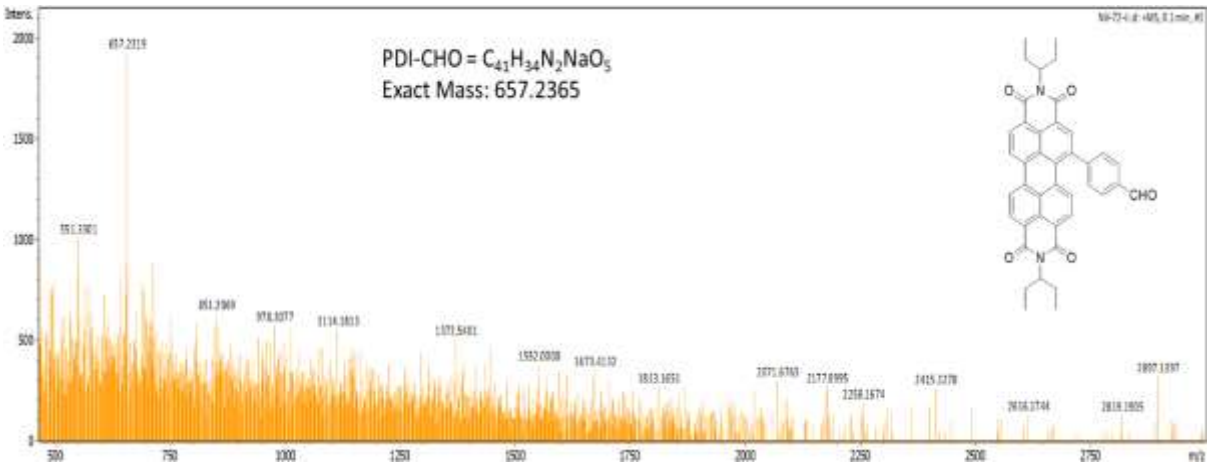

Figure S2c. Mass spectrum of PDI-CHO**.**

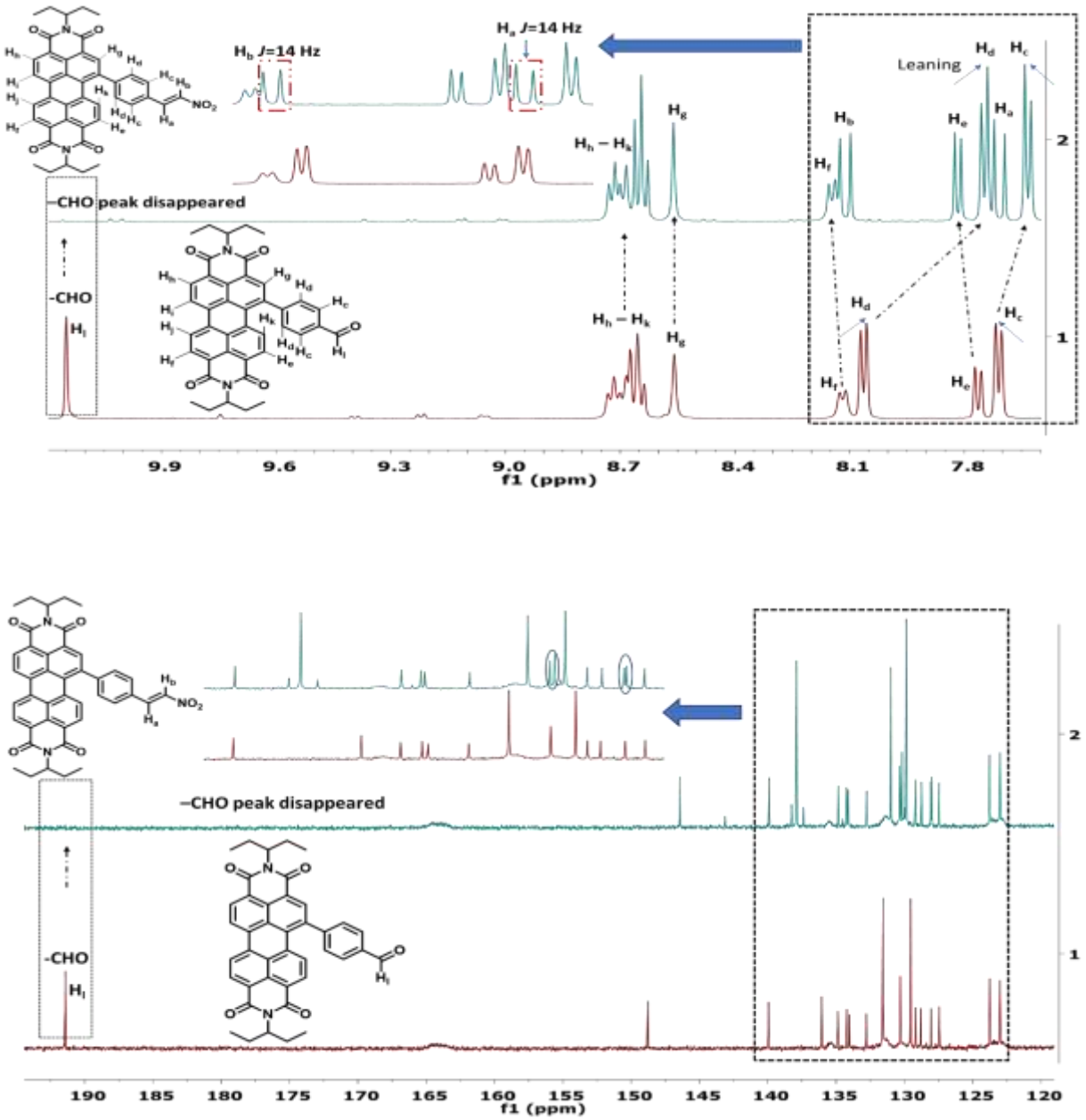

Figure S3: Partial ^{1}H (top) and ^{13}C (bottom) NMR stacked spectra of PDI **1** and PDI-CHO for comparison purpose to confirm the formation of PDI **1** from PDI-CHO.

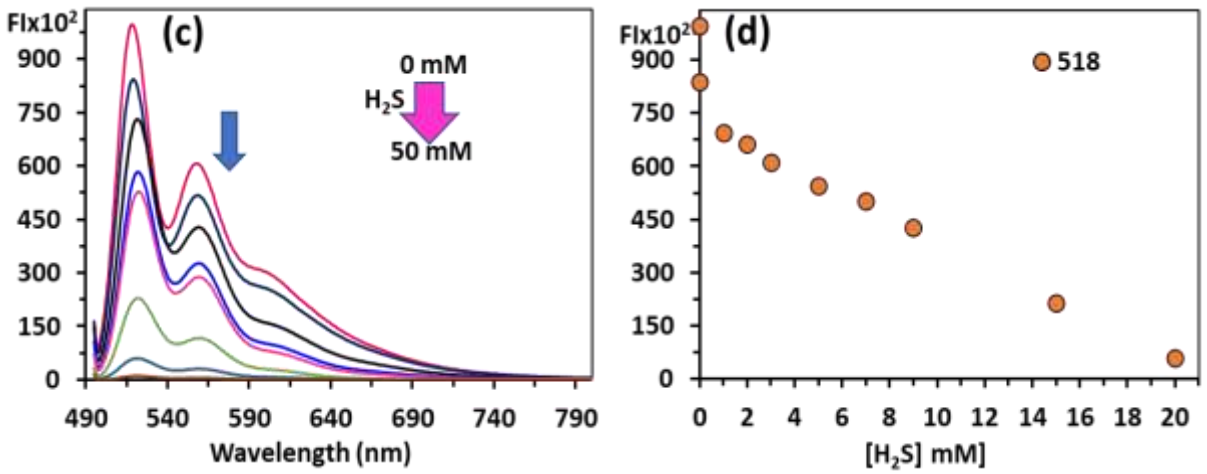

Figure S4. (a) Fluorescence spectra of neutral PDI **1** (10 µM) upon addition of different concentrations of H_2S (0–20 mM); (b) fluorescence intensity plot at different wavelengths against concentrations of H_2S.

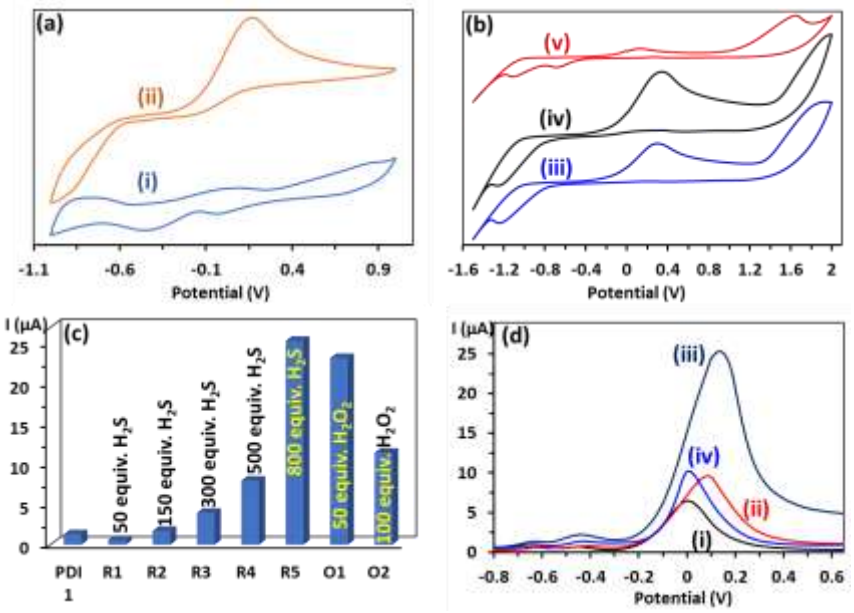

Figure S5. (a) The cyclic voltammetry (CV) of labels (i) neutral PDI **1** and (ii) neutral PDI **1**+30 mM H_2S; (b) The cyclic voltammetry (CV) of (iii) neutral PDI **1**+50 mM H_2S; (iv) neutral PDI **1**+80 mM H_2S; (v) neutral PDI **1**+30 mM H_2S+1 mM H_2O_2; (c) Change in current (I) value upon successive addition of different equivalents of H_2S in neutral PDI **1** followed by addition of H_2O_2; (d) Differential Pulse Voltammetry (DPV) of neutral PDI **1** upon addition of various concentrations of H_2S labelled as (i) 30 mM; (ii) 50 mM; (iii) 80 mM and upon addition of (iv) 1 mM H_2O_2 in neutral PDI **1**+80 mM H_2S solution.

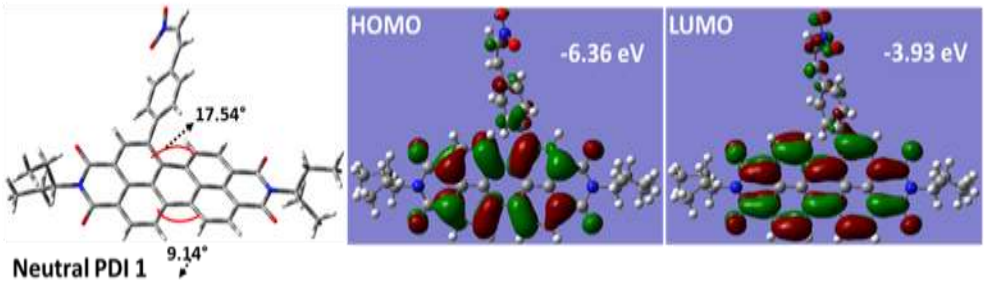

Figure S6. The density functional theory (DFT) calculations of neutral PDI **1** and PDI **1**$^{\cdot-}$ calculated using B3LYP with 6-31G(d) basis sets.

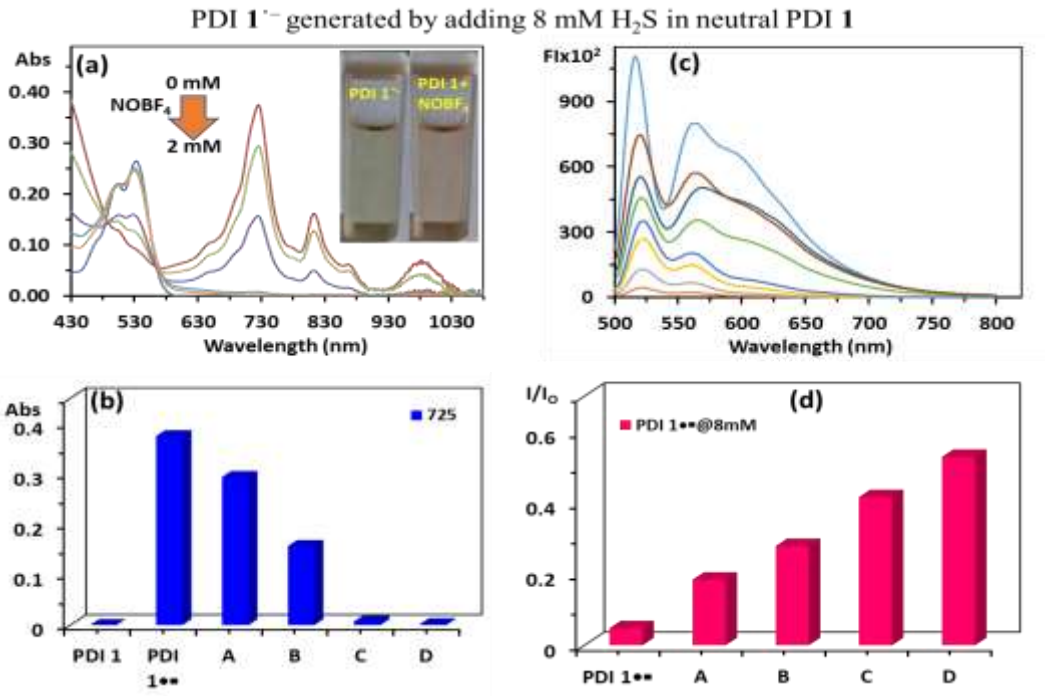

Figure S7. Effect of $NOBF_4$ on the (a,b) absorbance (c,d) emission spectra of PDI **1**$^{\cdot-}$ in-situ generated by addition of 8 mM concentrations of H_2S. The labels in Figure 5d stands for (A) = PDI **1**$^{\cdot-}$+0.5 mM $NOBF_4$; (B) = PDI **1**$^{\cdot-}$+1.5 mM $NOBF_4$; (C) = PDI **1**$^{\cdot-}$+3.0 mM $NOBF_4$; (D) = PDI **1**$^{\cdot-}$+5.0 mM $NOBF_4$.

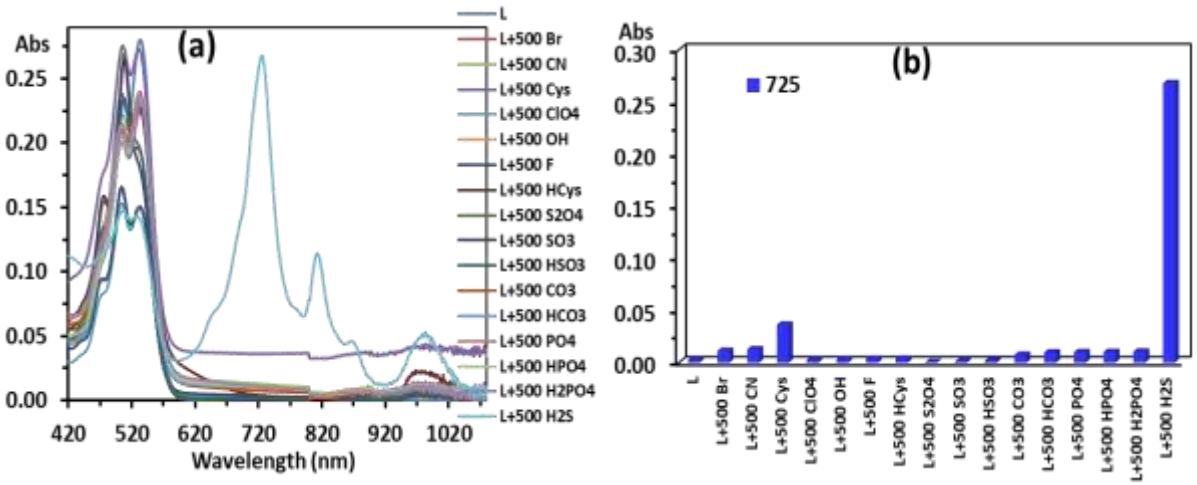

Figure S8. (a) Absorbance spectrum and (b) bar graph of PDI **1** upon addition of analytes (8 mM) recorded in 50% HEPES buffer–THF solution.

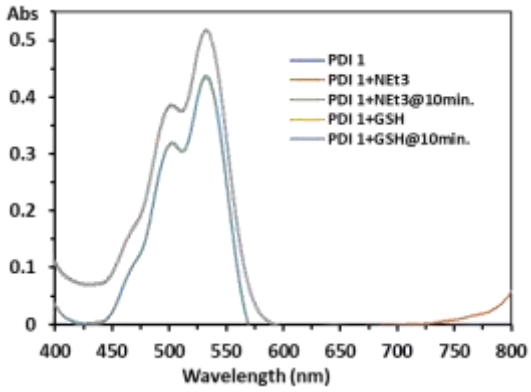

Figure S9. Absorbance spectra of PDI **1** (10 μM) recorded in 50% HEPES buffer–THF upon addition of different concentrations of triethylamine and glutathione (GSH) (8 mM).

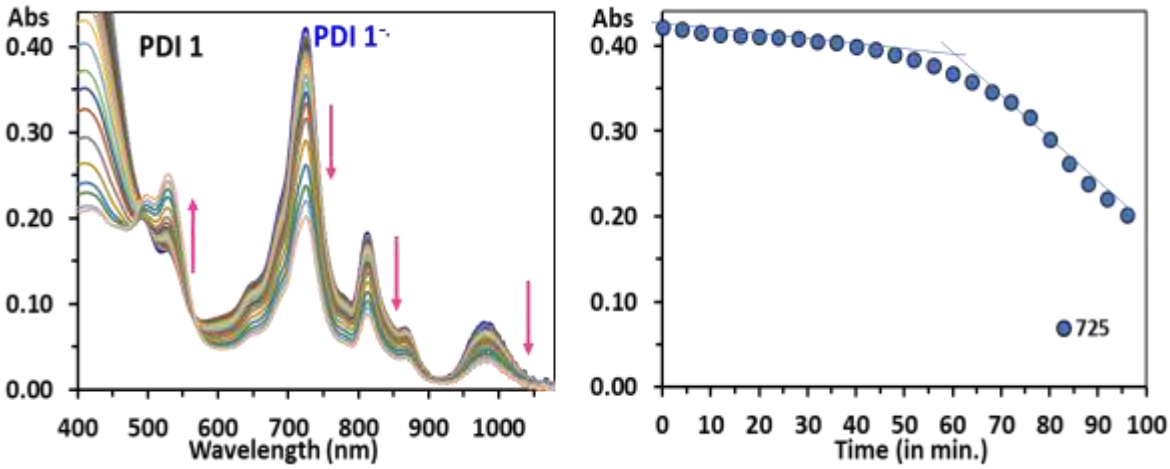

Figure S10. Absorbance spectra and absorbance intensity plot at 725 nm against the time to calculate the stability of the PDI $\mathbf{1}^{\bullet-}$ in hypoxic environment; All readings have been recorded in 50% HEPES buffer–THF.

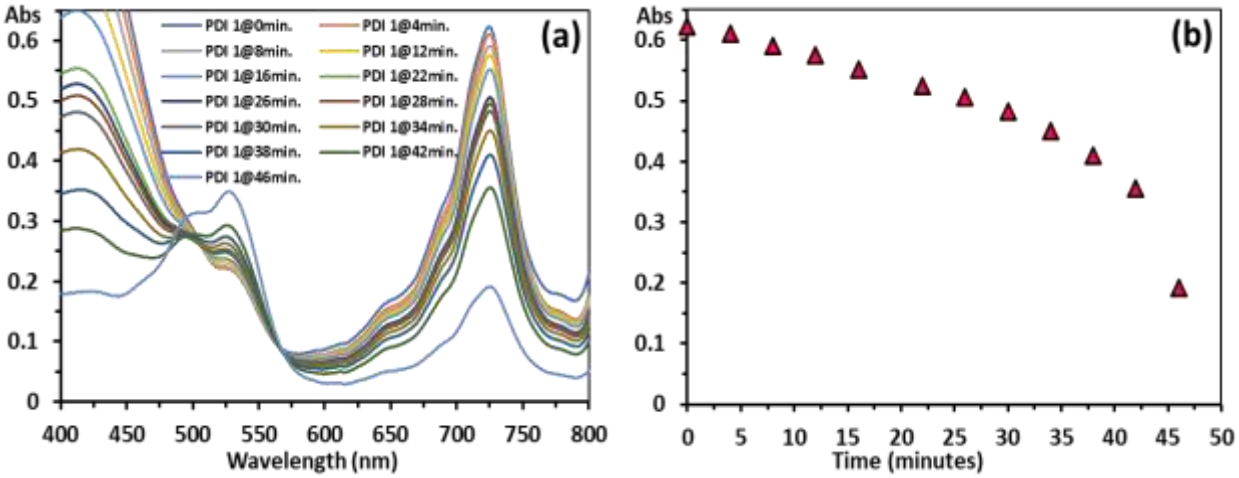

Figure S11. Absorbance spectra and absorbance intensity plot at 725 nm against the time to calculate the stability of the PDI $\mathbf{1}^{\bullet-}$ in normal oxygen environment; All readings have been recorded in 50% HEPES buffer–THF.

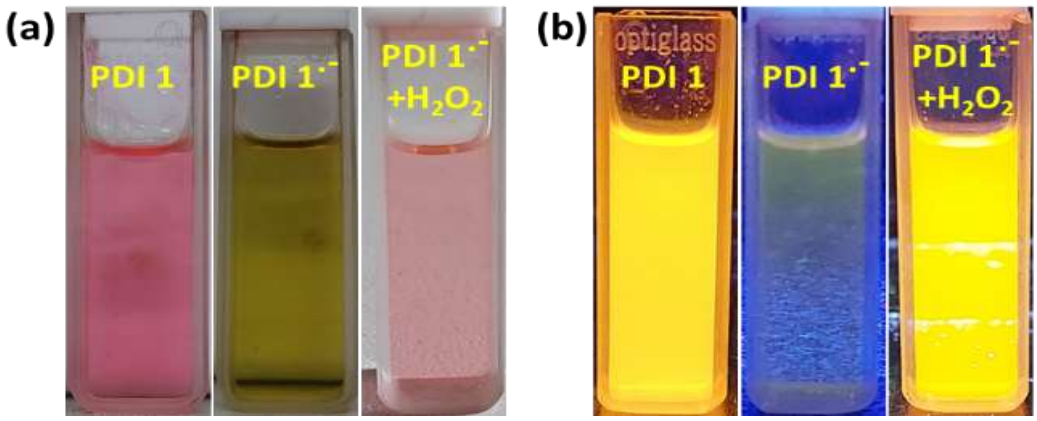

Figure S12. Photographs of PDI $\mathbf{1}^{\bullet-}$ before and after addition of H_2O_2 in (a) daylight and (b) 365 nm UV lamp.

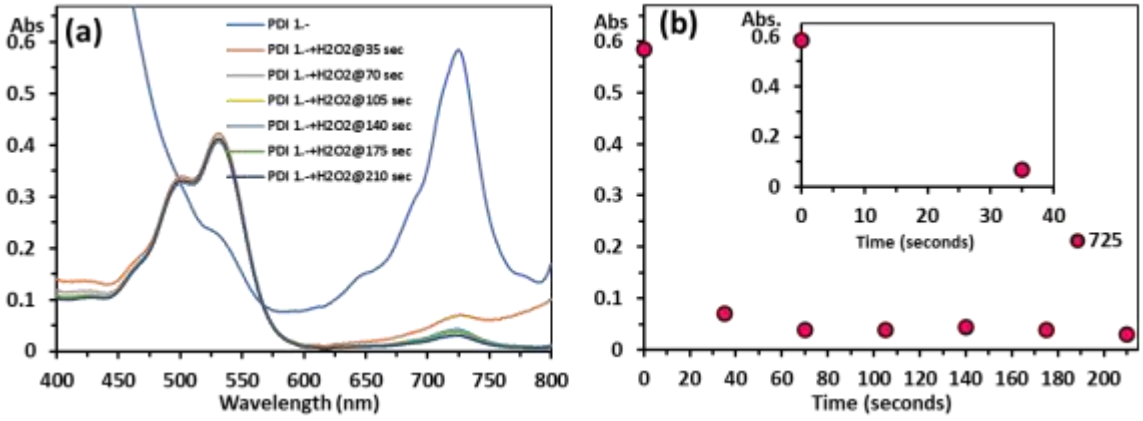

Figure S13. Absorbance spectra and absorbance intensity plot of PDI $\mathbf{1}^{\bullet-}$ + H_2O_2 (1 nM) at 725 nm against the time to calculate the response time. All readings have been recorded in 50% HEPES buffer–THF.

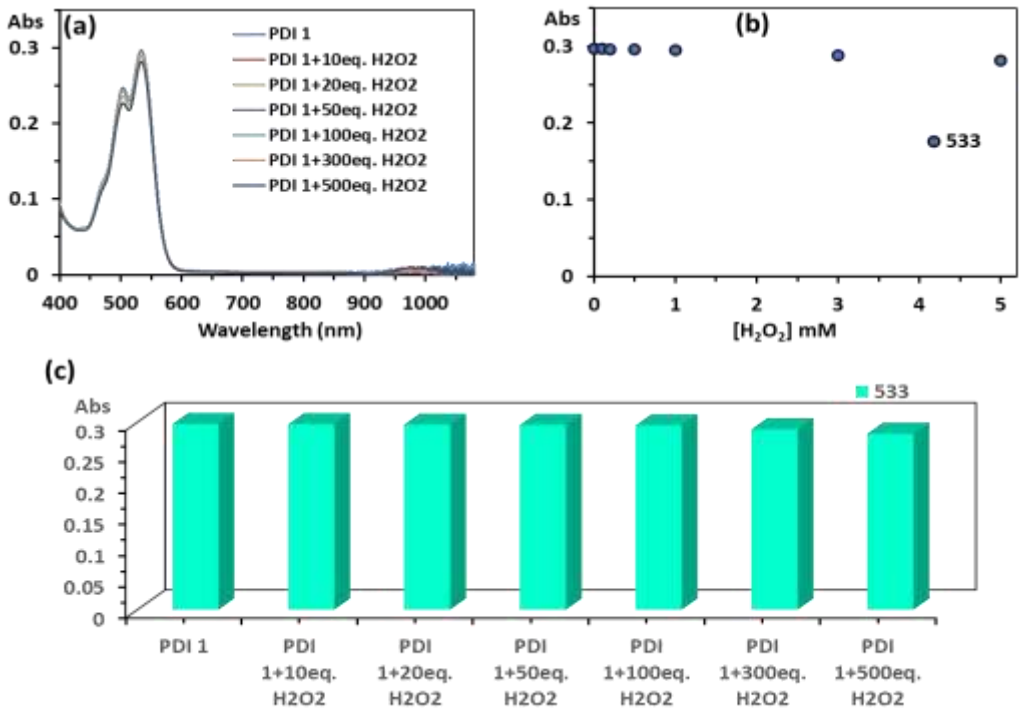

Figure S14. (a) Absorbance spectra; (b) absorbance intensity plot at 533 nm of neutral PDI **1** on addition of H_2O_2 and (g) bar graph showing the effect of H_2O_2 on PDI **1**. All readings have been recorded in 50% HEPES buffer–THF.

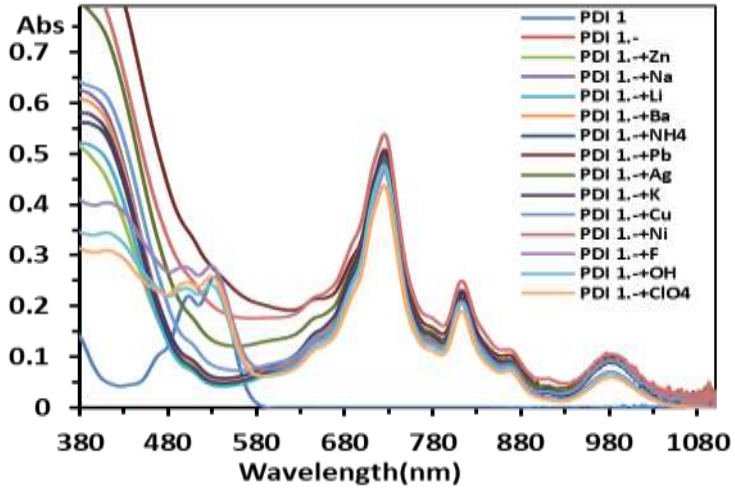

Figure S15. (a) Absorbance spectrum of PDI $\mathbf{1}^{\bullet-}$ upon addition of different analytes (metal ions 10 equiv. and anions 1 equiv.) to check the selectivity of the H_2O_2. All readings have been recorded in a 50% HEPES buffer–THF solution.

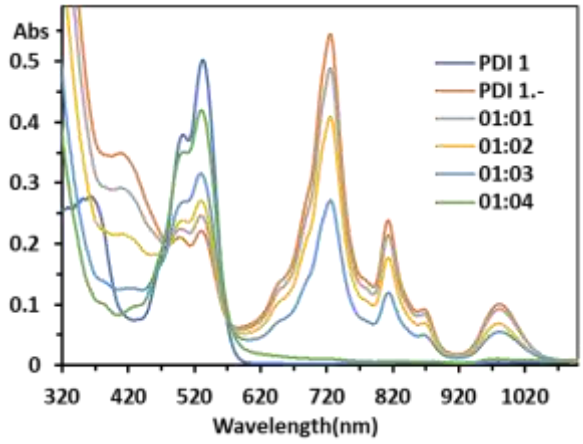

Figure S16. (a) Absorbance spectrum of PDI $\mathbf{1}^{\cdot-}$ upon addition of hydroxyl radical recorded in 50% HEPES buffer–THF solution. Hydroxyl radical has been generated in situ based on following reaction ($Fe^{2+} + H_2O_2 \rightarrow Fe^{3+} + OH^{\cdot-}$)[1]. The labels in the inset shows stochiometric ratio of H_2O_2 (0.1 nM) and Fe^{2+} (0.1 nM) as 01:01 (1:1); 01:02 (1:2); 01:03 (1:3); and 01:04 (1:4).

1. B. Lipinski, Hydroxyl radical and its scavengers in health and disease, Oxid. Med. Cell Longev, 2011, 2011, PMC 3166784